Lubrication studies of β-lactoglobulin-stabilized emulsions mixed with bovine submaxillary mucin

Hilal Yılmaz[1*], Ioannis S. Chronakis[2], Seunghwan Lee[3*]

[1]Department of Biotechnology, Bartın University, Kutlubey Campus, Bartın 74100, Türkiye

[2]DTU-Food, Research Group for Food Production Engineering, Laboratory of Nano-BioScience, Technical University of Denmark, Henrik Dams Allé, B202 2800 Kgs, Lyngby, Denmark

[3]Institute of Functional Surfaces, School of Mechanical Engineering, University of Leeds, LS2 9JT Leeds, United Kingdom

***Correspondence: hilalyilmaz@bartin.edu.tr**
S.Lee4@leeds.ac.uk

ABSTRACT

Understanding the oral processing of β-lactoglobulin (BLG)-stabilized emulsions is crucial for optimizing the physical and sensory attributes of colloidal food systems. This study investigates the tribological properties of BLG-stabilized emulsions and their mixtures with bovine submaxillary mucin (BSM) under various contact surfaces and testing conditions. Emphasis was placed on harmonizing tribological surfaces, including hydrophilic, hydrophobic, and roughened materials, to establish mechanistically supported generalized relationships under aligned testing conditions. Wettability measurements showed superior lubrication on hydrophilic steel surfaces, whereas hydrophobic materials (HDPE, PDMS, and rough PDMS) exhibited lower wettability and higher friction. Droplet size measurements using laser diffraction and optical microscopy revealed increased flocculation and the formation of larger droplet populations (~90 µm) upon BSM addition, indicating reduced emulsion stability. Pin-on-disk tribometry indicated increased coefficients of friction (COFs) in BSM-containing emulsions at low- and mid-speed regimes, likely due to hindered droplet entrainment and inter-droplet aggregation. At high speeds, COF differences diminished due to effective fluid entrainment. Investigations with various tribopairs revealed that hydrophobic and rough surfaces hindered fluid film formation, while hydrophilic–hydrophobic interfaces, such as steel–PDMS, enhanced lubrication even with mucin present. Mini-traction machine (MTM) tests demonstrated that BSM-containing emulsions maintained lubricity at high speeds under rolling/sliding conditions. However, insufficient viscosity and low contact pressure delayed the transition to elastohydrodynamic lubrication (EHL). These findings highlight the complex interplay between emulsion droplet size, surface characteristics, and mucin's amphiphilic and flocculation-promoting behavior in boundary lubrication. The study provides mechanistic insights into food tribology, aiding the design of emulsion-based food systems with improved mouthfeel and texture.

Keywords: β-lactoglobulin, emulsion, tribology, friction, mucin, wettability, microstructure

1. Introduction

Tribology has recently started to be established as a new approach to investigate oral processing of food in simulated oral environment (Chen & Stokes, 2012; Chen et al., 2014; Chojnicka-Paszun et al., 2012; Joyner Melito et al., 2014; Meyer et al., 2011; Prakash et al., 2013; Selway & Stokes, 2013; van Aken, 2013; Vardhanabhuti et al., 2011). Traditionally, rheological properties of foods have been correlated with some aspects of perceived texture in the mouth. However, bulk rheological properties alone do not represent all the in-mouth sensory properties for many soft-solid foods (Malone et al., 2003). Since food hydrocolloids and emulsions are often squeezed between moving surfaces such as the tongue and palate (or food substrate and palate) during eating, the texture or oral perception of food is related to its thin film rheological behavior as well as to its bulk properties (Chojnicka-Paszun et al., 2012; Malone et al., 2003; Meyer et al., 2011; Prakash et al., 2013; Selway & Stokes, 2013; Vardhanabhuti et al., 2011). Food tribology is becoming a prominent quantitative approach in numerous food physics laboratories worldwide. This technique involves assessing friction in the presence of model food structures such as aqueous hydrogels, emulsions, emulsion gels, micro-gels, as well as actual food products (Sarkar & Krop, 2019). Friction responses in food tribology depend on the surfaces in contact, applied load, and lubricant used etc. Apparently, the tribopairs in food tribology should represent various components of oral cavity involved in oral food consumption, such as tongue, teeth, or palate. However, replicating the soft, mucous-coated surface of the human tongue with common engineering materials poses challenges. An alternative is to employ animal tongues, such as pig tongues; while pig tongues share similar properties with human tongues, their use is limited by variability and rapid degradation (Sarkar et al., 2019). Harmonizing tribological surfaces and testing conditions is needed to develop generalized mechanistic relationships.

We are particularly interested in food emulsions in the context of food tribology because emulsion is important not only in food systems, such as salad dressing, but is also a long-standing subject in engineering tribology (Shewan et al., 2020). In the context of oral processing of food emulsions in simulated oral environment, saliva–emulsion interactions are anticipated to play an important role in understanding emulsion perception (van Aken et al., 2007). As both emulsions and saliva are intricate systems, applications of tribology techniques were started with quantitative characterization of the lubricating properties of the fluids involving saliva/model saliva and food proteins (Çelebioğlu et al., 2016; Vardhanabhuti et al., 2011; Çelebioglu et al., 2020).

Beta-lactoglobulin (BLG) stands out as a highly significant and extensively researched protein within dairy food systems. It serves as the predominant whey protein, making up over 50% of the total whey proteins present in bovine milk and commonly used as an emulsifier (Zúñiga et al., 2010). BLG is a crucial protein for nutritional intake during digestion and plays a pivotal role in shaping the physical and sensory characteristics of colloidal food systems, including emulsion stability, creaminess, and flavor release rate.

Human saliva is primarily composed of water (99.5%), various proteins (0.3%), small organic compounds, and inorganic salts, with a pH of approximately 6.8 (Zalewska et al., 2000). The main non-water component of saliva is mucin, a group of large extracellular glycoproteins composed of a linear polypeptide core with a highly glycosylated central part (Bansil & Turner 2006). Mucin is primarily responsible for the slipperiness of saliva and plays a crucial role in food oral processing and digestion, as it interacts with food components and affects sensory and textural properties (Svensson & Arnebrant, 2010).

Bovine submaxillary mucin (BSM) is commonly used as a model mucin in oral tribology studies due to its structural and functional resemblance to human salivary mucins, particularly MUC5B (Çelebioğlu et al., 2016; Sarkar et al., 2019). While whole human saliva is more relevant to actual oral processing, it is an extremely complex biological fluid, making it difficult to isolate and track the contributions of specific molecular components such as mucins. To overcome this complexity and improve experimental reproducibility, BSM is often selected as a simplified model to study mucin-related lubrication and interfacial interactions (Bongaerts et al., 2007; Sarkar et al., 2010). BSM is commercially available in a relatively purified form and exhibits a high degree of glycosylation and net negative charge at physiological pH, mimicking key physicochemical features of native salivary mucins under oral conditions.

The interactions of mucin with BLG have recently been investigated using spectroscopy, rheology, adsorption, and tribology (Çelebioğlu et al., 2015, 2016; Yılmaz et al., 2021). These studies revealed that BLG-mucin interactions significantly alter protein conformation, with pH influencing the stability and modulus of interfacial networks. Competitive displacement of BLG by mucin affects the viscoelastic properties of these layers.

In the present study, the tribological and physicochemical properties of a model mucus, namely highly concentrated negatively charged BSM, with the negatively charged BLG-stabilized emulsions (at pH 6.8) were investigated as an attempt to understand the physicochemical basis of the oral processing of BLG-stabilized emulsions. A main focus of this study was to investigate the influence of the composition of the emulsions, in particular, the oil:water ratio, BLG:oil ratio, and the effect of mucin. A unique feature of tribological parameters focused on this study was to vary the contacting interface in terms of hydrophilicity, hardness, and surface roughness by performing experiments at different tribopairs.

2. Materials and methods

2.1 Sample preparation

BLG from bovine milk was purchased from Sigma-Aldrich (L0130, Sigma-Aldrich A/S, Brøndby, Denmark) and BSM was purchased from Merck Millipore (M3895, Merck KGaA, Darmstadt, Germany) and both were used as received. Model mucus was formulated by utilizing BSM protein in

10 mM phosphate-buffered saline (PBS) at pH 6.8 to reach a final protein concentration of 3% (w/v) and stirring for 30 minutes at room temperature.

Emulsions were prepared using BLG protein solution and sunflower oil. A protein stock solution (1% w/v; 1 g BLG per 100 mL) was prepared by dispersing BLG in 10 mM PBS at pH 6.8 and stirring for 30 minutes at room temperature. To prepare BLG-stabilized emulsions, sunflower oil was initially added slowly to the protein solution while mixing with an Ultra-Turrax homogenizer (DI 25 basic; IKA-WERKE, Staufen, Germany) at a low speed (6,000 rpm). After all the sunflower oil had been added, the mixture was homogenized with the Ultra-Turrax at a high speed (20,000 rpm) for 30 minutes. A water bath was used during mixing to maintain a stable temperature (25°C), and sodium azide (0.02%) was added to prevent microbial growth.

To investigate the influence of adding model mucus on BLG-stabilized emulsions, BLG-stabilized emulsions have been prepared at different oil and protein concentrations. Afterwards, each BLG-stabilized emulsion was mixed with model mucus (3% (w/v) BSM solution) in such a way that the concentration ratio of BLG to BSM in the mixture was 1:1. In addition, to investigate the effect of adding mucin to emulsion, a BSM-added emulsion was also prepared using the same emulsion preparation formula as mentioned above. Lastly, reference samples, including sunflower oil, 1% (w/v) BLG solution, and 1% (w/v) BSM solution, were prepared for control purposes. PBS, used in the preparation of protein solutions, was measured independently and used as a reference. All the samples used, and their corresponding composition and/or preparation methods are listed in Table 1.

Table 1. Sample Notation and Corresponding Composition/Preparation Methods

Sample notation	Composition/Preparation of the samples
EB20	EB20 refers to an emulsion containing 20% v/v sunflower oil and 80% v/v water phase. The water phase is prepared as a 1% w/v BLG solution using PBS. Accordingly, the ratio of BLG protein to oil in the emulsion is 1:25 w/v.

EB20+M	EB20+M is the EB20 emulsion with 3% w/v BSM solution added.
EB30	EB30 refers to an emulsion containing 30% sunflower oil and 70% water phase. The water phase is prepared as a 1% w/v BLG solution. Accordingly, the ratio of BLG protein to oil in the emulsion is 1:43 w/v.
EB30*	EB30* is an emulsion with 30% sunflower oil and 70% water phase, like EB30. The water phase is a 1.71% w/v BLG solution to achieve a BLG to oil ratio of 1:25 w/v, matching EB20's protein to oil ratio.
EB30+M	EB30+M is the EB30 emulsion with 3% w/v BSM solution added.
EB30*+M	EB30*+M is the EB30* emulsion with 3% w/v BSM solution added.
EM20	EM20 refers to an emulsion containing 20% sunflower oil and 80% water phase, like EB20. However, the water phase is prepared as a 1% w/v BSM solution. The BSM to oil ratio is 1:25 w/v.
BLG	1% w/v BLG solution
BSM	1% w/v BSM solution
PBS	10 mM phosphate-buffered saline at pH 6.8

2.2 Tribology

Tribological properties of emulsions in this study have been conducted by employing combinations of various materials as tribopairs, including PDMS, HDPE, and steel. In particular, PDMS was fabricated to display very flat or rough surfaces to explore the influence of surface roughness. As both bulk mechanical properties (elasticity modulus and Poisson ratios) and surface roughness are critical parameters to affect the tribological properties, the values for tribopairs in tribometry experiments are listed in Table 2.

In addition, Hertzian contact pressure and composite surface roughness for the tribopairs in this study (including both PoD and MTM experiments below) are presented in Table 3. The surface roughness of roughened PDMS pin and disk, steel ball and HDPE ball for MTM was characterized with a laser profilometer by acquiring Ra values over 100 μm × 100 μm. Pin (PoD, rough). The surface roughness of other materials as cited from previous studies (see Table 2).

Table 2. Elasticity modulus, Poisson ratio, and surface roughness (Ra) of tribopair materials

	Elasticity modulus (GPa)	Poisson ratio	Surface roughness (R_a, nm)
PDMS	0.002[a]	0.5[a]	
Pin (PoD, smooth)			2 ± 0.5[a]
Disk (PoD, smooth)			0.5 ± 0.2[a]
Pin (PoD, rough)			4413 ± 473[b]
Disk (PoD, rough)			4836 ± 102[b]
Disk (MTM)			0.5 ± 0.2[b]
Steel			
Pin (PoD)	203[c]	0.3[c]	32[c]
Ball (MTM)	203[c]	0.3[c]	11[c]
HDPE			
Ball (MTM)	1[d]	0.42[d]	527 ± 143[b]

*a: (Lee and Spencer, 2005); b: laser profilometry; c: (Lee et al., 2003); d: (Lewis, 2003)

Table 3. Maximum contact pressure (under 1 N for PoD and 2 N for MTM) and composite surface roughness of the tribopairs in this study.

Tribopairs	Hertzian Contact Pressure (MPa)	Composite surface Roughness (nm)
PoD		
Smooth PDMS-PDMS	0.3	2.06
Roughened PDMS-PDMS	0.3	6546
Steel-PDMS	1.1	32
MTM		
HDPE/PDMS	0.3	11
Steel/PDMS	0.3	527

2.2.1 Pin-on-disk tribometry

Lubricating properties of the emulsions, emulsion-mucin mixtures, and protein solutions at sliding contacts were characterized by pin-on-disk tribometry (PoD) (CSM, Peseux, Switzerland). In this approach, a loaded spherical pin is allowed to form a contact on a plane disk. The motor-driven rotation of the disk generates interfacial friction forces between the pin and the disk. The applied load is controlled by dead weight and the friction forces generated during sliding contact are monitored by a strain gauge. The coefficient of friction, μ, is defined from the relationship;

$$\mu = F_{friction}/F_{load}$$

where $F_{friction}$ is the interfacial friction force and F_{load} is the load applied by dead weight.

Initially, 'smooth' PDMS was chosen as the tribopair for both pin (6 mm in diameter) and disk (30 mm in diameter and 5 mm in thickness). The pin and disk from PDMS were prepared with the PDMS kit (Sylgard 184, Dow Corning) according to a procedure described by Nikogeorgos et al. (2014). For smooth PDMS disk, the side exposed to air during curing was used. In addition to PDMS-PDMS tribopair, roughened PDMS pin and disk, and steel pin and PDMS disk were used as tribopairs. Roughened PDMS pins and disks were prepared by roughening the corresponding templates by means of sandblasting and the sides exposed to roughened surfaces of templates were used. To investigate the speed-dependent and load-dependent behavior of emulsions, a sliding speed range of 0.25 – 100 mm/s and loads of 1, 2, 5, 7, and 10 N were selected, respectively. The friction force data were collected for 100 rotations at room temperature (25 °C) and the tests were repeated multiple times. For each measurement, a tribopair of PDMS-PDMS (or any PDMS surface) was used only once and discarded to avoid cross contamination between measurements. However, steel pins were used again after cleaning. Steel pins were cleaned by means of ultrasonication in ethanol for 15 min. Steel pins/balls were further cleaned with a plasma cleaner (2 min, high power, Harrick Plasma) and used immediately after plasma treatment.

2.2.2 Mini traction machine (MTM)

Lubrication properties of the emulsions were characterized at mixed rolling/sliding contacts over a wider and higher speed range (mean speed, 10 – 1,200 mm/s) by means of a mini-traction machine (MTM, PCS Instruments Ltd., UK) too. Mixed rolling/sliding contacts are provided with MTM by independent rotation of ball and disk. The mean speed is defined as [$|speed_{ball}$ - $speed_{disk}|/2$]. The slide/roll ratio (SRR) is defined as SRR = ($|speed_{ball}$ - $speed_{disk}|$)/[($speed_{ball}$ + $speed_{disk}$)/2] × 100%, where 0% SRR represents pure rolling and 200% SRR represents pure sliding. In this study, SRR of 20% was employed in all measurements. Tests were conducted at room temperature (25 °C) with the tribopair consisting of HDPE ball–PDMS disk and steel ball–PDMS disk. The PDMS disks were prepared from the two-component silicone kit (Sylgard 184, Dow Corning), which was mentioned above, as well. A thick PDMS slab (ca. 5 mm) was cast on top of a steel disk (ca. 5 mm) for each sample. HDPE balls were purchased from a supplier (19.05 mm (¾ inch) in diameter, Precision Plastic Ball Co., IL) and were used as received. The steel ball (AISI 52100) was purchased from PCS Instruments. For each measurement, a new PDMS disk was employed, whereas the same HDPE and steel balls were used after cleaning as described above. The mechanical properties (elasticity modulus and Poisson ratio) of the tribopair materials are presented also in Table 2.

While the tribological surfaces used in this study did not replicate the papillae-like microstructure of the tongue, they were carefully selected to represent a range of hydrophilic, hydrophobic, and rough surface conditions. Simplified tribo-pair surfaces remain widely used in recent food tribology studies and offer reproducible platforms for formulation screening under controlled conditions (Kew et al., 2021; Hong et al., 2024; Du and Meng, 2023; You et al., 2023).

2.3 Contact angle – goniometer

Contact angle measurements were performed with a goniometer (Model Raméhart 200, Succasunna, NJ) and running software version 2.4.11. Static contact angles by distilled water were measured by applying a 5 μL droplet onto surfaces.

2.4 Rheology

The viscosity of the samples was examined using a controlled stress HAAKE™ MARS™ rheometer (Thermo Scientific Inc., Germany). Flow measurements using a coaxial cylinder set-up were performed in which the shear rate was increased from 10 to 100 s^{-1}. All measurements were carried out at room temperature (25 °C).

2.5 Droplet size and distribution

Droplet size distributions of the emulsions and emulsion-mucin mixtures were determined using a laser diffraction particle size analyzer (Mastersizer 2000, Malvern Instruments Ltd., UK). Measurements were performed at room temperature, and data were reported as volume-weighted mean diameters (D[4,3]).

Additionally, optical microscopy (Olympus U-LH100–3 microscope, Olympus Corporation, Tokyo, Japan) was used to visually assess the size and morphology of emulsion droplets before and after mucin addition.

2.6 Statistical Analysis

Data obtained in this study were expressed as the mean ± standard deviation of triplicate measurements. Data were statistically analyzed using SPSS software (version 28, IBM SPSS Inc., Armonk, NY, USA) with significance established at $p < 0.05$.

3. Results and Discussion

3.1. Wettability of emulsion-mucin systems on different contact surfaces

Wettability is a fundamental property that governs the interaction between liquid and solid surfaces, playing a critical role in understanding fluid behavior and surface compatibility. Measuring static contact angles provides valuable insights into how emulsions and emulsion-mucin mixtures interact with various surfaces, which is essential for evaluating their spreading, adhesion, and stability characteristics. To characterize this behavior, static contact angles of the emulsions and emulsion-mucin mixtures were measured, as summarized in Table 4. The wettability of the emulsion samples varied significantly across the tested surfaces, with the lowest contact angle values observed on the steel surface. This behavior cannot be solely attributed to steel's hydrophilicity, as steel's unique property allows it to be wetted by both oil and water. This feature facilitates better fluid spreading and the formation of a continuous liquid film, contributing to uniform surface coverage.

In contrast, the hydrophobic surfaces, HDPE, PDMS, and rough PDMS, exhibited higher contact angles, reflecting lower wettability compared to steel. Among these hydrophobic surfaces, HDPE showed slightly better wettability, as evidenced by lower contact angle values compared to PDMS and rough PDMS. The similar contact angle values for PDMS and rough PDMS suggest that surface roughness did not significantly influence wettability; however, the slightly higher values for rough PDMS indicate that surface roughness may have amplified the hydrophobic effect without completely altering the spreading behavior of the emulsions.

Table 4. Contact angles of different emulsion droplets and their mucin mixtures on different tribopair surfaces

Surface	Sample	Contact Angle (°)
PDMS	Water	100±1.5
	EB20	87.1±2.8

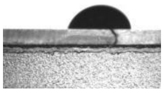	EB20+M	92.0±1.5
	EB30	91.0±1.7
	EB30+M	89.7±2.2
HDPE	Water	90±1.5
	EB20	61.0±2.1
	EB20+M	59.8±2.5
	EB30	56.3±2.8
	EB30+M	57.5±2.4
Rough PDMS	Water	110±1.5
	EB20	91.5±1.2
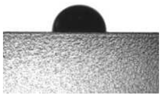	EB20+M	89.4±1.9
	EB30	91.9±1.3
	EB30+M	90.7±1.8
Steel	Water	65±1.5
	EB20	3.7±3.1
	EB20+M	12.1±4.2
	EB30	18.0±4.7
	EB30+M	17.1±5.1

3.2 Droplet size and microstructure of emulsions and emulsion-mucin mixtures

The assessment of droplet size and microstructure is crucial for understanding the fundamental stability and morphology of emulsions and emulsion-mucin mixtures. These measurements provide insight into the effects of mucin addition on emulsion characteristics, such as droplet size distribution, flocculation, and coalescence, which directly influence their physical behavior and overall stability.

The volume-based droplet size distributions of the oil-protein emulsions with and without mucin (BSM) are presented in Fig. 1. Two major peaks, one in ca. 0.05–1.00 µm and the other in ca. 10–100 µm, were observed. The smaller droplet population was observed in the EB30 and EB30* emulsions with a peak maximum around 0.1 µm, and in EB20 with a peak maximum around 0.2 µm. Upon addition of BSM, the major small-sized droplets disappeared and larger droplet populations (10–200 µm, with a peak maximum around 90 µm) emerged instead. The distribution was somewhat narrower for EB20+M compared to EB30 and EB30*. Lastly, it should be noted that minor populations of smaller droplets (0.05–20 μm) and larger droplets (1–80 μm) were still present across all samples, reflecting the inherent inhomogeneity in droplet size.

Upon the addition of BSM, the emulsions exhibited a main peak around 90 μm, which is significantly larger than typical BSM or BSM clusters. BSM typically ranges in size from 0.1 to 1 μm, as shown in previous studies where BSM (catalog number M3895) was used as received, and a mucin solution was prepared in 30 mM NaCl (Bastardo et al., 2002). Thus, these data support that BSM molecules are either at the interface between water and oil droplets acting as an emulsifier or promoting flocculation between droplets (Sarkar et al., 2010). Additionally, a small portion of BSM may exist in the aqueous phase, as indicated by minor peaks in the 0.1–1 μm range, also shown in Fig. 1.

In parallel with the laser diffraction-based size distribution measurements, droplet morphology was examined using microscopy (Fig. 2). These images show a somewhat broader droplet size distribution in EB20+M compared to EB20. However, a more striking difference is the enhanced emulsion flocculation induced by mucin. Although the size of aggregated or flocculated droplets in EB20+M is difficult to quantify due to their irregular shapes, the enhanced flocculation likely reduces Brownian motion and contributes to the observed increase in larger droplet populations (around 90 μm) (Fig. 1).

There are several reasons why oil droplets increase in size upon the addition of BSM (Fig. 1 and Fig. 2). Firstly, if BSM acts at the interface in place of BLG, its larger molecular size and bulk may yield larger droplets. Secondly, BSM's higher molecular weight compared to BLG results in lower mobility, which may impair the formation of smaller droplets and facilitate coalescence.

Mucin has film-forming properties, and its introduction might result in the creation of an additional layer around emulsion droplets. This mucin film could modify the interactions between droplets, potentially promoting aggregation and leading to larger droplet sizes. Moreover, BLG is known to be sensitive to changes in pH and ionic strength (Majhi et al., 2006). The addition of mucin may influence the electrostatic balance at the droplet interfaces, reducing repulsive forces and facilitating droplet aggregation. Although this suggests that electrostatic interactions play a role, the dominant mechanism governing these changes remains uncertain due to the complex nature of the system's charge distribution. Sarkar et al. (2010) reported that the addition of porcine gastric mucin (PGM, Type III, bound sialic acid 0.5–1.5%), which carries a net negative charge at neutral pH, caused increased flocculation, despite the fact that BLG-stabilized emulsion droplets are also negatively charged at this pH. This indicates that the observed flocculation is unlikely due to simple electrostatic attraction and may rather involve depletion flocculation or mucin-mediated bridging effects. In addition to electrostatic interactions, the observed flocculation upon mucin addition may also be influenced by depletion attraction and bridging mechanisms, as mucin is a highly charged anionic polyelectrolyte. According to classical colloid theory and recent findings (Dickinson, 2019; Feng et al., 2023), the presence of non-adsorbing high molecular weight polymers in the continuous phase can induce attractive forces between droplets by generating an osmotic pressure imbalance. This depletion force can overcome long-range electrostatic repulsions and lead to accelerated aggregation or network formation in emulsion systems. Such interactions have been well-documented in O/W emulsions stabilized by proteins and polysaccharides (Han et al., 2024). Therefore, it is plausible that BSM not only contributes to interfacial adsorption but also facilitates droplet flocculation via depletion attraction and bridging, resulting in the formation of larger droplet aggregates as observed in both droplet size distribution and microscopy images.

Furthermore, it is plausible that BSM not only contributes to interfacial adsorption but may also facilitates droplet flocculation via depletion attraction and bridging, resulting in the formation of larger droplet aggregates as observed in both droplet size distribution and microscopy images (Ritzoulis et al., 2012). Another study demonstrated that negatively charged mucin (PGM) readily interacted with positively charged lactoferrin-stabilized emulsion droplets, achieving a mucin coverage of approximately 1 mg/m². In contrast, for BLG-stabilized emulsions, which also bear a net negative charge at pH 6.8, mucin coverage was lower (0.6 mg/m² surface load) under the same conditions, suggesting weaker interactions (Sarkar et al., 2009). While BLG-stabilized emulsions remained stable, depletion flocculation was observed at higher mucin concentrations (≥1.0 wt%) (Sarkar et al., 2009). Given these findings, BSM appears to act primarily by stabilizing emulsions through interfacial and flocculation-related mechanisms (e.g., steric hindrance or bridging), rather than by significantly reducing interfacial tension like classical low-molecular-weight surfactants.

3.3 Boundary lubricating properties: pin-on-disk tribometry

3.3.1 Influence of model mucus on the speed dependent lubricating properties of emulsions

The coefficients of friction (COFs) for the sliding contacts of PDMS-PDMS in different emulsion samples were measured using a PoD at various loads (1, 2, 4, 6, 8, and 10 N). The results showed that all emulsions exhibited no meaningful dependence on the applied load (data not shown). Therefore, subsequent tribological measurements, focused on speed dependency, were conducted under a constant load of 1 N for all samples.

Fig. 3 illustrates the COFs of the smooth PDMS-PDMS tribopair in emulsions, emulsion-mucin mixture systems, and control fluids across varying speeds (from 0.25 to 100 mm/sec) under a 1 N load. Fig. 3a presents the changes in the COFs as a function of speed for BLG-stabilized emulsions and their mixtures with BSM. The data indicate that all emulsions exhibit similar COFs profiles, with a decrease beginning from at around 0.5 to 1 mm/sec, followed by a plateau extending to 100 mm/sec. Upon adding mucin to the emulsions, a significant increase in their COFs was observed in the low- and mid-speed ranges. However, the COFs of the emulsion-BSM mixtures rapidly decreased as the speed increased and thus the difference between emulsions with or without mucins disappeared in the high-speed regime (≥ 50 mm/sec). This is ascribed to effective entrainment of fluids at very high speeds.

These lubrication trends can be further understood by considering the interplay between wettability (Section 3.1) and microstructure (Section 3.2). The superior wettability of emulsions on hydrophilic surfaces promotes fluid spreading and film formation, which can reduce COFs in boundary lubrication regimes, as will be discussed below (Section 3.3.2). However, on hydrophobic surfaces, such as PDMS, the limited wettability hinders fluid-film formation, resulting in higher COFs. Additionally, the microstructural changes induced by mucin—particularly the formation of larger, flocculated droplets—contribute to reduced droplet mobility and hindered entrainment into the contact zone during sliding. These combined factors can explain the higher COFs observed for emulsion-mucin mixtures at low-to-mid speeds. At high speeds, fluid entrainment becomes dominant, and the effects of surface wettability and microstructure diminish, resulting in similar COFs for emulsions with and without mucin.

The contributions of individual components to these behaviors were further explored in Fig. 3b and Fig. 3c. Fig. 3b compared the COFs of all reference fluid, while Fig. 3c evaluated the lubricating behavior of EM20 (an emulsion prepared with BSM instead of BLG) to examine the influence of mucin without BLG.

The results show that the COF changes of BLG-stabilized emulsions were very similar to those of sunflower oil, which supports that the oil component of the emulsion was primarily responsible for lubrication at the tribological interface, even in oil-in-water (O/W) emulsions although water is the dominant phase. In contrast, water-based fluids without oils, including PBS and BLG solution, did not effectively lubricate hydrophobic surfaces such as PDMS. Poor lubricity of BLG as aqueous lubricant additive has been demonstrated in our previous study too (Çelebioğlu et al., 2016). Although BLG is amphiphilic, it lacks distinct hydrophobic patches or hydrophilic blocks due to too small molecular weight and size and thus does not contribute to the aqueous lubrication of PDMS-PDMS tribological interface. On the other hand, mucin is an effective additive for aqueous lubrication, particularly for hydrophobic interfaces (Lee at al., 2005). It is notably efficient at lubricating hydrophobic and soft surfaces like PDMS-PDMS. The superior lubricity of BSM aligns with previous studies that demonstrate its effective boundary lubrication at a PDMS-PDMS interface, even under much lower load and speed (Çelebioğlu et al., 2016; Nikogeorgos et al., 2014).

Nevertheless, the addition of BSM to emulsions rather deteriorated their lubricating properties (Fig. 3a). First of all, this implies that the added BSM molecules do not effectively migrate and adsorb onto the PDMS–PDMS interface to reduce the friction in the emulsions. As mentioned above, this is likely due to the tribological interface being dominated by the oil phase. Secondly, it is important to note that the COFs of emulsions rather increased, as opposed to being simply unaffected, upon addition of BSM. One possible explanation is that BSM, being amphiphilic, may act as a macromolecular emulsifier, potentially altering the stabilization of oil droplets. Although we did not directly measure interfacial displacement or competitive adsorption in this study, it is possible that BSM could associate with or partially replace BLG at the oil–water interface, resulting in altered interfacial composition and droplet interactions. Both mucin and BLG are known to exhibit interfacial activity at the oil–water interface, though they differ in their mechanisms. Mucin, due to its amphiphilic and highly glycosylated structure, can act as a surface-active agent, reducing interfacial tension and forming a viscoelastic film that stabilizes emulsions (Shi et al., 1999; Vingerhoeds et al., 2005; Chang and McClements, 2016). In contrast, BLG stabilizes emulsions primarily by adsorbing at the interface and forming a structured protein film, whose properties depend on its conformation and interactions with other components (Sarkar et al., 2009; Sarkar et al., 2010; Zhai et al., 2011). The interplay between mucin and BLG at the interface may affect interfacial structure, droplet size distribution, and consequently, lubrication behavior (Brown et al., 2021).

Previous studies have shown that mucins exhibit interfacial activity and may adsorb at oil–water interfaces, though their adsorption behavior and competitive dynamics with globular proteins such as BLG are still under investigation (Sarkar et al., 2016; Nikogeorgos et al., 2015; Sarkar & Krop, 2019; Çelebioğlu et al., 2017). Alternatively, BSM may act as a bridging agent between emulsion droplets, promoting flocculation (Sarkar et al., 2010). In either case, such interactions could increase the average droplet size (see Section 3.2) and hinder the entrainment of oil droplets into the contact zone during sliding. The observation that EM20 in Figure 3c exhibited a similar trend to the emulsion–mucin mixtures, although with overall slightly lower COF values, further supports BSM's role in altering the interfacial and structural properties of the emulsions (Fig. 3c).

Although friction coefficients appeared largely independent of applied normal load (1–10 N), this observation is based solely on tribological measurements. Post-friction microstructural analysis of the emulsions was not performed in the present study and would be necessary to determine whether structural destabilization or droplet coalescence occurred under higher mechanical stress. Similarly, in BSM-containing emulsions where increased droplet size was associated with higher COFs, it remains possible that partial rupture of large droplets occurred during sliding, potentially altering lubrication behavior through oil release. These mechanisms cannot be confirmed within the scope of the current study but represent important directions for future investigation.

3.3.2 Influence of contact interfaces

In order to investigate the influence of material parameters of tribopairs, such as surface roughness, surface hydrophilicity, and bulk mechanical properties, several different tribopairs were employed. In addition to the contact pressure and composite surface roughness shown in Table 3, the contact angles of the tribopair surfaces with the emulsion samples were presented in Table 4.

Firstly, the smooth PDMS pin and disks were switched with a roughened pair. No change in bulk mechanical properties is expected, but a slight increase in surface hydrophobicity is observed due to increased surface roughness on hydrophobic surface (Sabbah et al., 2016). The load and speed were identical to those for smooth PDMS-PDMS interface. Different emulsions and each of their BSM mixture (see Table 1) are shown separately in Fig. 4a, 4b, and 4c, while the reference liquids are shown in Fig. 4d.

In general, surface roughness has two opposing effects on the friction forces of hydrophobic interface. Firstly, as the hydrophobic interaction between two surfaces across contacting area, i.e., adhesion, can contribute to the friction forces, surface-roughening may reduce the adhesion and friction forces due to reduced *real* area of contact. On the contrary, shear strength can increase for roughened surfaces due to increasing asperity contacts. Furthermore, the possibility of forming fluid lubricants at the interface is retarded at roughened interface (see below for further discussion).

The findings from Section 3.1 on wettability provide valuable context for understanding the lubrication behavior discussed in this section. Surfaces with high hydrophilicity, such as steel, demonstrated superior wettability (low contact angles) and correspondingly lower COFs, indicating effective fluid-film formation and lubrication. Conversely, hydrophobic surfaces like PDMS and rough PDMS, which showed high contact angles, exhibited inhibited fluid spreading and retarded fluid-film formation, leading to increased COFs dominated by asperity contacts. These results highlight the critical role of surface hydrophilicity and roughness in governing both wettability and lubrication performance of emulsion and emulsion-mucin systems.

Additionally, the destabilizing effect of mucin, as observed in Section 3.2, is exacerbated in modulating lubrication for roughened surfaces. The larger, flocculated droplets in emulsion-mucin mixtures become even more difficult to entrain into the contact zone leading to increased friction. This effect is particularly prominent at low speeds, where boundary lubrication dominates, and fluid entrainment is minimal. On smooth PDMS surfaces, the smaller asperity contacts combined with lower surface roughness allow for improved droplet entrainment and spreading, partially mitigating the destabilizing effects of mucin. However, the influence of mucin remains evident, as flocculation hinders the mobility of droplets, reducing their ability to lubricate the interface effectively.

Which factor plays the more dominant role depends on the detailed hydrophobicity and surface roughness. In this study, in comparison to the smooth PDMS-PDMS tribopairs, no significant differences were observed in the COF vs speed plots for reference liquids (Fig. 4d). Nonetheless some noticeable changes were observed from the emulsion samples and their mixtures with BSM. For instance, the COFs did not substantially decrease with increasing speed for EB20 (Fig. 4a) and rather increased for EB30 and EB30* (Fig. 4b and 4c). Moreover, for all the emulsion samples, mixing with BSM did not lead to any appreciable changes in COFs. For all the possible effects from surface roughening mentioned above, the retarded formation of fluid formation appears to be the most dominant in this case. It is stressed that the activation of fluid-film lubrication is not determined by the fluid film thickness alone, but also by composite surface roughness, $s = \sqrt{s_{ball}^2 + s_{disk}^2}$ where s = composite surface roughness, s_{ball} = surface roughness of ball, s_{disk} = surface roughness of disk, as well; normally, it is accepted that the fluid film lubrication is activated when the fluid film thickness is at least 3 times higher than the composite surface roughness (Hutchings and Shipway, 2017) and the required ratio could be even larger for elastic interfaces (De Vicente et al., 2006). As shown in Table 2 and 3, the roughened PDMS pin and disk have a Ra value of ca. 4.4-4.8 μm that the composite surface roughness is more than 3,000 times higher than that of smooth PDMS-PDMS contact. A fluid film possibly formed between this roughened pair of PDMS surfaces is practically ignorable and thus, the roughened PDMS-PDMS interface is most likely to be dominated by asperity contacts over the entire speed range even in fluid solution. This can account for a solid-like contact characteristics, namely increasing COF with increasing speed, for rough PDMS-PDMS interface. Moreover, as fluid does not contribute to the lubrication, whether the droplets are stabilized by BLG or mucin, or even BLG/mucin together, the influence of adding BSM into the BLG-stabilized emulsion becomes also ignorable.

Since EB20, EB30, and EB30* showed very similar COFs for all the tribopairs investigated so far, namely PDMS-PDMS and roughened PDMS interfaces, some of forthcoming experiments were conducted with the EB20 only.

A significant concern in oral tribology experiments involving polymeric materials as tribopair, is their intrinsic surface hydrophobicity unlike the hydrophilic nature of saliva-coated tongue surfaces in real-life scenarios (Sarkar et al., 2019). To investigate the friction behavior at an interface involving hydrophilic surface, a hydrophilic-hydrophobic tribopair was further employed, namely steel-PDMS tribopair (Fig. 5). At this pair, both the emulsion (EB20) and emulsion-BSM mixture (EB20+M) showed very low COFs (≤ 0.05) over the entire speed range. This can be ascribed to that "clean" bearing steel (AISI 52100) is both hydrophilic and lyophilic (contact angle $< 5°$ for both, see the Table 4) and is well lubricated by both fluids (Fig. 4b). In a way, steel/PDMS pair is an ideal interface that emulsion can readily lubricate because both oil phase and water phase can effectively lubricate both or one surface at least. This can also explain how EB20+M sustained low COFs values over the entire speed range (Fig. 4a). Even though addition of BSM to EB20 can disrupt the stability of the emulsion as in hydrophobic interfaces, availability of either oil or aqueous phases can still lubricate the interface in an effective way.

3.4 Fluid-lubrication properties: Mini-traction machine (MTM)

3.4.1 Rheological properties of model mucus

Fluid-film lubrication properties are often correlated to the rheological properties of fluids in question. As shown in Fig. 6, both EB20 and EB20+M showed a Newtonian behavior within the shear rate range of 10 to 100 s^{-1}, and this signifies that the viscosity of the emulsions remains constant over this range of shear rates. More importantly, the apparent viscosity of the EB20+M was nearly twice than that of the EB20. This is expected due to the increased concentration of macromolecules in the emulsion. Furthermore, as addressed above (Section 3.2), BSM molecules may also facilitate flocculation of the emulsions leading to an enhanced viscosity of the EB20.

Moreover, the ability of the saliva protein mucin to change the COF and the viscosity of food emulsions can be attributed to its unique molecular structure and functional characteristics. Mucin is a glycoprotein that is characterized by its large, complex, and heavily glycosylated structure. When introduced into food emulsions, mucin molecules can contribute to an increase in viscosity by creating a more viscous and resistant medium. The entanglement and hydration of mucin molecules within the emulsion can impede the flow of the liquid, leading to higher viscosity.

Moreover, mucin has film-forming capabilities, and it can coat the surfaces of emulsion droplets, forming a protective layer as mentioned above. This film formation can contribute to an increase in viscosity by altering the internal structure of the emulsion and providing resistance to flow.

3.4.2 Lubrication properties of the emulsions at mixed rolling/sliding

A fixed load (2 N) was applied with the estimated Hertzian contact pressure of 0.3 MPa. A force of 2 N enables the application of minimal contact pressure, and this is significant in oral processing contexts.

The lubricating properties of EB20 and its mixture with mucin (EB20+M) were further investigated at a mixed rolling/sliding contact by employing HDPE ball–PDMS tribopair on MTM. In the present measurement settings, MTM is significantly easier to lubricate compared to PoD. As the highest speed was increased to 1 m/s and the dominant contact characteristic was rolling than sliding, a possibility to form fluid film lubricant at the interface is expected to be much higher than

PoD tribometry (pure sliding) shown in the previous section. The results for EB20 and EB20+M in addition to the reference samples are presented in Fig. 7. In general, EB20+M showed somewhat higher COF values than EB20, except for very high-speed regime (ca. > 500 mm/s) where both samples showed similar COF values. The COF values for EB20 in low-speed regime were similar to those of sunflower oil, although both emulsions showed clearly higher COF values than sunflower oil at higher speeds (> ca. 200). Similarly with the PoD results (Figure 3), the destabilizing effects of mucin, highlighted by the increased droplet sizes and flocculation, contribute to higher COFs at lower speeds. These structural changes hinder the entrainment of droplets into the contact zone, reducing lubrication efficiency in the boundary regime. At higher speeds, as fluid entrainment dominates, the influence of mucin-induced flocculation diminishes, and the lubrication performance of emulsions with and without mucin converges. This shift from structure-dominated to entrainment-dominated lubrication mirrors the trends observed in the PoD experiments (Section 3.3.1) but is more pronounced under rolling/sliding conditions in MTM. Additionally, the larger droplets in EB20+M, while initially detrimental to lubrication, are more effectively incorporated into the fluid film at high speeds, highlighting the dynamic interplay between structural and hydrodynamic factors. On the contrary, PBS (Ghosh et al., 2014) and BLG solutions showed distinctly higher COF values compared to other samples, similarly with the results from PoD experiments, and they revealed an increasing trend with increasing speed.

In a study conducted by Taylor and Mills (2020), emulsion samples consisting of 20%, 30%, and 50% vegetable oil, along with pure water and pure oil samples, were utilized for MTM tests. They noted that pure oil exhibited a nearly perfect Stribeck curve, displaying distinct regimes with smooth transitions, and the emulsions showed a comparable friction response. Generally, it is suggested that oil is the primary lubricating component in emulsions at low-speed regimes, while water begins to be entrained at high-speed regimes (Taylor and Mills, 2020). This phenomenon applies to both PoD and

MTM data, as well as to the overall comparison of PoD data versus MTM data. For example, the addition of BSM to the emulsion deteriorated the lubricating properties as measured by PoD, but not by MTM. This is likely due to the fact that MTM operates under near pure rolling conditions where the entrainment of fluid into the contact zone is substantially easier for both water and oil phases. Overall, the MTM results showed limited differentiation among samples with or without BSM. Previous tribological data from Malone et al. (2003), investigating emulsions, closely align with the findings presented here, where boundary and mixed lubrication were observed for oil emulsions, while mixed and elastohydrodynamic lubrication (EHL) were noted for pure oil.

Fig. 8 shows the results for the same experiments as Fig. 7 however a steel ball-PDMS tribopair was used. Due to hydrophilic characteristics of steel ball, the COF values were much lower than those from HDPE-PDMS tribopair for both EB20 and EB20+M. The emulsion containing mucins (EB20+M) displayed somewhat lower COF values than the emulsion without mucin (EB20), but only at very low speeds. At speeds beyond 10 mm/s, COFs of emulsion and emulsion-mucin mixture showed similar values with each other as well as with the reference samples, i.e. PBS and oil. This is also a reflection of facile entrainment as well as enhanced wetting of the interface with both water and oil phase-based fluids.

Despite the enhanced lubrication by the emulsions at steel/PDMS interface, it is notable that a transition to EHL in COF was not evident up to the highest speed (Fig. 8). The absence of a transition to EHL in this study can be attributed to the experimental conditions employed. EHL typically requires high fluid viscosity, elevated contact pressures (>500 MPa), and shear rates between 10^5 to 10^7 s^{-1} to induce a pressure-driven viscosity increase, forming a thick fluid film that elastically deforms the interacting surfaces (Hutchings and Shipway, 2017). However, in this study, the applied contact pressure (0.3 MPa) and constant Newtonian viscosity observed across the tested shear rate range were insufficient to meet these conditions (De Vicente et al., 2006). While 0.3 MPa is representative of oral processing, it did not induce significant elastic deformation of the tribological surfaces, even at the highest rolling/sliding speed of 1 m/s.

Additionally, the low viscosity of the emulsions constrained fluid-film thickness, further preventing the transition to EHL, which aligns with prior observations with low-viscosity lubricants (Lee et al., 2021; Soltanahmadi et al., 2022). Gmür et al. (2021) similarly reported that in low-viscosity systems, the insufficient film thickness hinders the transition to EHL, with friction reduction primarily governed by surface interactions rather than viscosity-driven mechanisms.

Conversely, studies where EHL transitions occur typically involve emulsions with significantly higher viscosities, enabling thicker fluid films under elevated pressures and shear rates. For example, Soltanahmadi et al. (2022) observed that low-viscosity systems exhibit delayed EHL transitions, whereas higher viscosities enhance film thickness, facilitating earlier EHL onset. Similarly, Douaire et al. (2014) showed that low-viscosity oil-continuous emulsions form thinner films, limiting EHL formation, whereas increasing the phase volume and dynamic viscosity enhances fluid entrainment and film thickness. Additionally, Perrino et al. (2024) demonstrated that enhanced hydration results in thicker fluid films, which contribute to improved lubrication performance.

These findings highlight the critical role of viscosity in promoting EHL, as higher viscosities are essential for maintaining sufficient film thickness and fluid entrainment under shear conditions. They also align with the nature of oral tribology, where low viscosities and contact pressures, typical of saliva and food systems, hinder EHL formation. Despite the absence of EHL, this study provides critical insights into boundary and fluid-film lubrication mechanisms. It emphasizes the role of droplet size, wettability, and fluid entrainment in modulating lubrication behavior under realistic oral processing conditions. Thus, these findings further evaluate the effect of low-viscosity emulsions on oral processing and tribological behavior.

3.5 Comparative Summary of Tribological Approaches

This study employed two complementary tribological platforms — PoD tribometer and a MTM — to explore the lubrication behavior of BLG-stabilized emulsions and their mixtures with BSM under different surface and motion conditions.

The PoD system was used to assess boundary lubrication performance across a wide range of sliding speeds (0.25–100 mm/s) under a constant load of 1 N. This platform enabled investigation the effects of surface-dependent parameters (e.g., wettability and roughness) and allowed for controlled evaluation of frictional behavior as a function of emulsion composition. Notably, the PoD setup emphasized sliding contact on hydrophobic and hydrophilic surfaces, which is particularly relevant for mimicking localized contact zones in oral processing.

In contrast, the MTM system enabled the study of lubrication behavior under rolling–sliding conditions, which facilitates the fluid entrainment into the contact zone, especially in high-speed regime. The MTM provided insight into frictional transitions across lubrication regimes, particularly highlighting how BSM-containing emulsions maintained low friction at higher entrainment speeds, despite not achieving full EHL due to their low viscosity.

Overall, both platforms showed consistent trends: (1) the addition of BSM increased friction at low-to-intermediate speeds due to droplet flocculation and hindered entrainment, and (2) these differences were minimized at higher speeds where fluid entrainment became dominant. The use of both PoD and MTM tribometers thus provided a more robust and comprehensive understanding of emulsion lubrication mechanisms under diverse contact conditions relevant to food oral processing.

4. Conclusion

In conclusion, the lubricating behavior of various oil-in-water emulsions stabilized using BLG, and the effect of BSM model mucus (mucin), revealed a complex and dynamic relationship between various factors, including speed, load, contact interfaces, rheological properties, droplet size, and microstructure. The COF values of the emulsions generally exhibited little dependence on the load; however, the sliding speed played a crucial role, as well as the choice of tribopair materials with different hydrophobicity of the contacting surfaces.

The results revealed that wettability of the emulsions is highly surface-dependent, with hydrophilic steel surfaces providing a favorable condition for lubrication, while hydrophobic surfaces, such as HDPE and PDMS, were less effective due to reduced fluid spreading. Interestingly, surface roughness of PDMS did not significantly alter wettability, suggesting that other factors, such as emulsion composition, play a more dominant role. The addition of BSM caused significant droplet aggregation and flocculation, resulting in larger, heterogeneous droplets. These changes deteriorated emulsion stability and increased friction at low to moderate speeds in boundary lubrication regimes. However, at higher speeds, fluid entrainment mitigated these differences. Furthermore, in addition to interfacial adsorption, BSM may contribute to droplet flocculation through mechanisms such as depletion attraction and polymer bridging, which are consistent with the formation of larger droplet aggregates observed in both size distribution and microscopy analyses. The observed increase in viscosity in BSM-containing emulsions further highlights the effect of mucin altering the rheological and structural properties and thereby influencing the lubrication performance of emulsions. However, this increase in viscosity remained insufficient to support the transition to EHL conditions.

Overall, this work highlights the importance of understanding the interplay between surface properties, emulsion composition, and testing conditions in determining the frictional properties of emulsion systems. The findings offer valuable insights for understanding and manipulating the frictional behavior of emulsions, paving the way for potential applications in diverse fields such as food science and tribology, among others. However, further experimental investigation is warranted to assess the potential structural changes under frictional stress, including droplet rupture or oil release, particularly in BSM-containing emulsions.

CRediT authorship contribution statement

Hilal Yılmaz: Conceptualization, Methodology, Formal analysis, Visualization, Writing – original draft, Writing – review & editing. **Ioannis S. Chronakis**: Conceptualization, Supervision, Writing – review & editing. **Seunghwan Lee**: Conceptualization, Methodology, Visualization, Supervision, Writing – review & editing

Declaration of competing interest

There are no conflicts of interest to declare.

Acknowledgment

The authors thank the Independent Research Fund Denmark (DFF, Project 3164-00092B) for financial support and the Republic of Türkiye Ministry of National Education for the PhD scholarship.

References

Bansil, R., & Turner, B. S. (2006). Mucin structure, aggregation, physiological functions and biomedical applications. *Current Opinion in Colloid & Interface Science*, *11*(2-3), 164-170. https://doi.org/10.1016/j.cocis.2005.11.001

Bastardo, L., Claesson, P., & Brown, W. (2002). Interactions between mucin and alkyl sodium sulfates in solution. A light scattering study. *Langmuir*, *18*(10), 3848-3853. https://doi.org/10.1021/la015717u

Bongaerts, J. H. H., Rossetti, D., & Stokes, J. R. (2007). The lubricating properties of human whole saliva. *Tribology Letters*, *27*, 277-287. https://doi.org/10.1007/s11249-007-9232-y

Brown, F. N., Mackie, A. R., He, Q., Branch, A., & Sarkar, A. (2021). Protein–saliva interactions: a systematic review. *Food & Function,* 12(8), 3324-3351. https://doi.org/10.1039/D0FO03180A

Çelebioğlu, H. Y., Gudjónsdóttir, M., Chronakis, I. S., & Lee, S. (2016). Investigation of the interaction between mucins and β-lactoglobulin under tribological stress. *Food Hydrocolloids, 54*, 57-65. https://doi.org/10.1016/j.foodhyd.2015.09.013

Çelebioğlu, H. Y., Gudjónsdóttir, M., Meier, S., Duus, J. Ø., Lee, S., & Chronakis, I. S. (2015). Spectroscopic studies of the interactions between β-lactoglobulin and bovine submaxillary mucin. *Food Hydrocolloids, 50*, 203-210. https://doi.org/10.1016/j.foodhyd.2015.04.026

Çelebioğlu, H. Y., Kmiecik-Palczewska, J., Lee, S., & Chronakis, I. S. (2017). Interfacial shear rheology of β-lactoglobulin—Bovine submaxillary mucin layers adsorbed at air/water interface. *International Journal of Biological Macromolecules*, *102*, 857-867. https://doi.org/10.1016/j.ijbiomac.2017.04.063

Çelebioğlu, H. Y., Lee, S., & Chronakis, I. S. (2020). Interactions of salivary mucins and saliva with food proteins: A review. *Critical reviews in food science and nutrition, 60*(1), 64-83. https://doi.org/10.1080/10408398.2018.1512950

Chang, Y., & McClements, D. J. (2016). Characterization of mucin–lipid droplet interactions: Influence on potential fate of fish oil-in-water emulsions under simulated gastrointestinal conditions. *Food Hydrocolloids*, 56, 425-433. https://doi.org/10.1016/j.foodhyd.2015.12.034

Chen, J., & Stokes, J. R. (2012). Rheology and tribology: Two distinctive regimes of food texture sensation. *Trends in Food Science & Technology, 25*(1), 4–12. https://doi.org/10.1016/j.tifs.2011.11.006

Chen, J., Liu, Z., & Prakash, S. (2014). Lubrication studies of fluid food using a simple experimental set up. *Food Hydrocolloids, 42*, 100–105. https://doi.org/10.1016/j.foodhyd.2014.01.003

Chojnicka-Paszun, A., de Jongh, H. H. J., & de Kruif, C. G. (2012). Sensory perception and lubrication properties of milk: Influence of fat content. *International Dairy Journal, 26*, 15–22. https://doi.org/10.1016/j.idairyj.2012.04.003

De Vicente, J., Stokes, J.R., & Spikes, H.A. (2006). Soft lubrication of model hydrocolloids. *Tribology International*, 39(12), 1246-1257. https://doi.org/10.1016/j.foodhyd.2005.04.005

Dickinson, E. (2019). Strategies to control and inhibit the flocculation of protein-stabilized oil-in-water emulsions. *Food hydrocolloids*, *96*, 209-223. https://doi.org/10.1016/j.foodhyd.2019.05.021

Douaire, M., Stephenson, T., & Norton, I. T. (2014). Soft tribology of oil-continuous emulsions. *Journal of Food Engineering, 139*, 24-30. https://doi.org/10.1016/j.jfoodeng.2014.04.007

Du, L., & Meng, Z. (2023). Oleofoams and emulsion foams stabilized by sodium stearoyl lactylate: Insight into their relations based on microstructure, rheology and tribology. *Food Hydrocolloids*, 137, 108317. https://doi.org/10.1016/j.foodhyd.2022.108317

Feng, G., Wang, G., Li, Q., Han, C., Wei, D., Guo, J., ... & Yang, X. (2023). Depletion attraction driven formation of Spirulina emulsion gels for 3D printing. *Food Hydrocolloids*, 141, 108691. https://doi.org/10.1016/j.foodhyd.2023.108691

Ghosh, S., Choudhury, D., Das, N. S., & Pingguan-Murphy, B. (2014). Tribological role of synovial fluid compositions on artificial joints—a systematic review of the last 10 years. Lubrication Science, 26(6), 387-410. https://doi.org/10.1002/ls.1266

Gmür, T. A., Mandal, J., Cayer-Barrioz, J., & Spencer, N. D. (2021). Towards a Polymer-Brush-Based friction modifier for oil. *Tribology Letters, 69*(4), 124. https://doi.org/10.1007/s11249-021-01496-w

Han, C., Feng, G., Yin, S., Wang, G., Wang, J., Wan, Z., ... & Yang, X. (2024). Stabilization of oil-water interface by non-interfacial adsorbed native starch granules using depletion attraction. *Food Hydrocolloids*, 156, 110330. https://doi.org/10.1016/j.foodhyd.2024.110330

Hong, J. S., Kim, M. R., Choi, Y. J., Lee, I. Y., Chun, Y. G., Jang, H. W., & Kim, B. K. (2024). Tribological properties of real foods using extended Stribeck curves and their relationship with nutritional and rheological parameters. *Journal of Texture Studies*, 55(4), e12857. https://doi.org/10.1111/jtxs.12857

Hutchings, I.M., & Shipway, P. (2017). *Tribology: Friction and Wear of Engineering Materials.* Elsevier.

Joyner Melito, H. S., Pernell, C. W., & Daubert, C. R. (2014). Impact of formulation and saliva on acid milk gel friction behavior. *Journal of Food Science, 79*, 67–80. https://doi.org/10.1111/1750-3841.12439

Junkar, I. (2016). Interaction of cells and platelets with biomaterial surfaces treated with gaseous plasma. In *Advances in Biomembranes and Lipid Self-Assembly* (Vol. 23, pp. 25-59). Academic Press. https://doi.org/10.1016/bs.abl.2016.01.002

Kew, B., Holmes, M., Stieger, M., & Sarkar, A. (2021). Oral tribology, adsorption and rheology of alternative food proteins. *Food Hydrocolloids*, 116, 106636. https://doi.org/10.1016/j.foodhyd.2021.106636

Lee, R. T., Yang, K. T., Chiou, Y. C., & Lin, Y. T. (2021). Thermal effect on a mixture lubrication with oil-in-water emulsions in ehl contacts. *Tribology Transactions*, *64*(2), 202-213. https://doi.org/10.1080/10402004.2020.1820122

Lee, S., Müller, M., Ratoi-Salagean, M., Vörös, J. Pasche, S., De Paul, S. M., Spikes, H. A., Textor, M., Spencer, N. D. (2003), Boundary lubrication of oxide surfaces by poly(L-lysine)-*g*-poly(ethylene glycol) (PLL-*g*-PEG) in Aqueous Media. *Tribology Letters*, 15, 231-239. https://doi.org/10.1023/A:1024861119372

Lee, S., Müller, M., Rezwan, K., & Spencer, N. D. (2005). Porcine gastric mucin (PGM) at the water/poly (dimethylsiloxane)(PDMS) interface: influence of pH and ionic strength on its conformation, adsorption, and aqueous lubrication properties. *Langmuir, 21*(18), 8344-8353. https://doi.org/10.1021/la050779w

Lee, S., Spencer, N. D. (2005), Aqueous lubrication of polymers: Influence of surface modification. *Tribology International*, 38(11-12), 922-930. https://doi.org/10.1016/j.triboint.2005.07.017,

Lewis, G. (2003), Finite element analysis of a model of a therapeutic shoe: effect of material selection for the outsole, *Bio-Medical Materials and Engineering*, 13, 75–81.

Majhi, P. R., Ganta, R. R., Vanam, R. P., Seyrek, E., Giger, K., & Dubin, P. L. (2006). Electrostatically driven protein aggregation: β-lactoglobulin at low ionic strength. *Langmuir*, *22*(22), 9150-9159. https://doi.org/10.1021/la053528w

Malone, M. E., Appelqvist, I. A. M., & Norton, I. T. (2003). Oral behaviour of food hydrocolloids and emulsions. Part 1. Lubrication and deposition considerations. *Food Hydrocolloids, 17*(6), 763-773. https://doi.org/10.1016/S0268-005X(03)00097-3

Meyer, D., Vermulst, J., Tromp, R. H., & de Hoog, E. H. A. (2011). The Effect of inulin on tribology and sensory profiles of skimmed milk. *Journal of Texture Studies, 42*, 387–393. https://doi.org/10.1111/j.1745-4603.2011.00298.x

Nikogeorgos, N., Madsen, J. B., & Lee, S. (2014). Influence of impurities and contact scale on the lubricating properties of bovine submaxillary mucin (BSM) films on a hydrophobic surface. *Colloids and Surfaces B: Biointerfaces, 122*, 760-766. https://doi.org/10.1016/j.colsurfb.2014.08.017

Perrino, C., Lee, S., & Spencer, N. D. (2024). Quantitative Comparison of the Hydration Capacity of Surface-Bound Dextran and Polyethylene Glycol. *Langmuir, 40*(27), 14130-14140. https://doi.org/10.1021/acs.langmuir.4c01582

Prakash, S., Tan, D. D. Y., & Chen, J. (2013). Applications of tribology in studying food oral processing and texture perception. *Food Research International, 54*, 1627–1635. https://doi.org/10.1016/j.foodres.2013.10.010

Ritzoulis, C., Siasios, S., Melikidou, K. D., Koukiotis, C., Vasiliadou, C., & Lolakos, S. (2012). Interactions between pig gastric mucin and sodium caseinate in solutions and in emulsions. *Food Hydrocolloids*, *29*(2), 382-388. https://doi.org/10.1016/j.foodhyd.2012.04.005

Sabbah, A., Youssef, A., & Damman, P. (2016). Superhydrophobic surfaces created by elastic instability of PDMS. *Applied Sciences*, *6*(5), 152. https://doi.org/10.3390/app6050152

Sarkar, A., & Krop, E. M. (2019). Marrying oral tribology to sensory perception: A systematic review. *Current Opinion in Food Science, 27*, 64-73. https://doi.org/10.1016/j.cofs.2019.05.007

Sarkar, A., Andablo-Reyes, E., Bryant, M., Dowson, D., & Neville, A. (2019). Lubrication of soft oral surfaces. *Current Opinion in Colloid & Interface Science, 39*, 61-75. https://doi.org/10.1016/j.cocis.2019.01.008

Sarkar, A., Goh, K. K., & Singh, H. (2009). Colloidal stability and interactions of milk-protein-stabilized emulsions in an artificial saliva. *Food Hydrocolloids*, *23*(5), 1270-1278. https://doi.org/10.1016/j.foodhyd.2008.09.008

Sarkar, A., Goh, K. K., & Singh, H. (2010). Properties of oil-in-water emulsions stabilized by β-lactoglobulin in simulated gastric fluid as influenced by ionic strength and presence of mucin. *Food Hydrocolloids*, *24*(5), 534-541. https://doi.org/10.1016/j.foodhyd.2009.12.005

Selway, N., & Stokes, J. R. (2013). Insights into the dynamics of oral lubrication and mouth feel using soft tribology: Differentiating semi-fluid foods with similar rheology. *Food Research International, 54*, 423–431. https://doi.org/10.1016/j.foodres.2013.07.044

Shewan, H. M., Pradal, C., & Stokes, J. R. (2020). Tribology and its growing use toward the study of food oral processing and sensory perception. Journal of texture studies, 51(1), 7-22. https://doi.org/10.1111/jtxs.12452

Shi, L., Miller, C., Caldwell, K. D., & Valint, P. (1999). Effects of mucin addition on the stability of oil–water emulsions. *Colloids and Surfaces B: Biointerfaces*, 15(3-4), 303-312. https://doi.org/10.1016/S0927-7765(99)00096-X

Soltanahmadi, S., Murray, B. S., & Sarkar, A. (2022). Comparison of oral tribological performance of proteinaceous microgel systems with protein-polysaccharide combinations. *Food Hydrocolloids, 129*, 107660. https://doi.org/10.1016/j.foodhyd.2022.107660

Svensson, O., & Arnebrant, T. (2010). Mucin layers and multilayers—Physicochemical properties and applications. *Current Opinion in Colloid & Interface Science*, *15*(6), 395-405. https://doi.org/10.1016/j.cocis.2010.05.015

Taylor, B. L., & Mills, T. B. (2020). Using a three-ball-on-plate configuration for soft tribology applications. *Journal of Food Engineering*, *274*, 109838. https://doi.org/10.1016/j.jfoodeng.2019.109838

van Aken, G. A. (2013). Acoustic emission measurement of rubbing and tapping contacts of skin and tongue surfaces in relation to tactile perception. *Food Hydrocolloids, 31*, 325–331. https://doi.org/10.1016/j.foodhyd.2012.11.020

van Aken, G. A., Vingerhoeds, M. H., & de Hoog, E. H. (2007). Food colloids under oral conditions. *Current Opinion in Colloid & Interface Science, 12*(4), 251-262. https://doi.org/10.1016/j.cocis.2007.07.011

Vardhanabhuti, B., Cox, P. W., Norton, I. T., & Foegeding, E. A. (2011). Lubricating properties of human whole saliva as affected by β-lactoglobulin. *Food Hydrocolloids, 25*(6), 1499-1506. https://doi.org/10.1016/j.foodhyd.2011.02.021

Vingerhoeds, M. H., Blijdenstein, T. B., Zoet, F. D., & van Aken, G. A. (2005). Emulsion flocculation induced by saliva and mucin. *Food Hydrocolloids*, 19(5), 915-922. https://doi.org/10.1016/j.foodhyd.2004.12.005

Wang, P., Chai, X., Chen, C., Duan, X., Wu, K., & Fu, X. (2024). Enhanced in vitro bioavailability of resveratrol-loaded emulsion stabilized by β-lactoglobulin-catechin with excellent antioxidant activity. *International Journal of Biological Macromolecules*, *267*, 131304. https://doi.org/10.1016/j.ijbiomac.2024.131304

Yılmaz, H., Lee, S., & Chronakis, I. S. (2021). Interactions of β-lactoglobulin with bovine submaxillary mucin vs. porcine gastric mucin: the role of hydrophobic and hydrophilic residues as studied by fluorescence spectroscopy. *Molecules, 26*(22), 6799. https://doi.org/10.3390/molecules26226799

You, K. M., Murray, B. S., & Sarkar, A. (2023). Tribology and rheology of water-in-water emulsions stabilized by whey protein microgels. *Food Hydrocolloids*, 134, 108009. https://doi.org/10.1016/j.foodhyd.2022.108009

Zalewska, A., Zwierz, K., Zółkowski, K., & Gindzienski, A. (2000). Structure and biosynthesis of human salivary mucins. *Acta Biochimica Polonica*, 47(4), 1067–1079. https://doi.org/10.18388/abp.2000_3960

Zhai, J., Wooster, T. J., Hoffmann, S. V., Lee, T. H., Augustin, M. A., & Aguilar, M. I. (2011). Structural rearrangement of β-lactoglobulin at different oil–water interfaces and its effect on emulsion stability. *Langmuir,* 27(15), 9227-9236. https://doi.org/10.1021/la201483y

Zúñiga, R. N., Tolkach, A., Kulozik, U., & Aguilera, J. M. (2010). Kinetics of formation and physicochemical characterization of thermally-induced beta-lactoglobulin aggregates. *Journal of Food Science*, 75(5), 261–268. https://doi.org/10.1111/j.1750-3841.2010.01617.x

FIGURE CAPTIONS

Fig. 1. Volume-based droplet size distribution of BLG-stabilized emulsions with and without mucin (BSM), measured by laser diffraction.

Fig. 2. Optical microscopy images of (a) EB20 after 30 minutes from emulsion preparation and (b) EB20+M after 5 minutes from mucin addition. The dotted area in (a) designates uniform, small-sized emulsion droplets, while the dotted area in (b) indicates larger, flocculated droplet clusters formed after mucin incorporation.

Fig. 3. Speed-dependent COF measurements at the PDMS-PDMS interface (1 N load) using Pin-on-Disk tribometry: (a) BLG-stabilized emulsions with/without mucin, (b) Reference samples: BLG and BSM solutions, sunflower oil, and buffer, (c) BLG vs. BSM stabilized emulsion

Fig. 4. Speed-dependent COF measurements at the Roughened PDMS-PDMS interface (1 N load) using Pin-on-Disk tribometry: **(a)** BLG-stabilized emulsion (EB20) with/without mucin, **(b)** BLG-stabilized emulsion (EB30) with/without mucin, **(c)** BLG-stabilized emulsion (EB30*) with/without mucin, **(d)** BSM stabilized emulsion (EM20) and reference solutions (BLG, OIL, PBS).

Fig. 5. Speed-dependent COF measurements at the Steel-PDMS interface (1 N load) using Pin-on-Disk tribometry: **(a)** BLG-stabilized emulsion (EB20) with/without mucin, **(b)** BSM stabilized emulsion (EM20) and reference solutions (BLG, OIL, PBS).

Fig. 6. Effect of the shear rate on the apparent viscosity of the EB20 with/without mucin

Fig. 7. Speed dependent friction coefficient measurement of BLG stabilized emulsion - with/without mucin (EB20, EB20+M), BSM stabilized emulsion (EM20), and reference samples (BLG, OIL) at HDPE-PDMS interface with Mini Traction Machine (MTM) (2 N load)

Fig. 8. Speed dependent friction coefficient measurement of BLG stabilized emulsion - with/without mucin (EB20, EB20+M), BSM stabilized emulsion (EM20), and reference samples (BLG, OIL, PBS) at Steel-PDMS interface with Mini Traction Machine (MTM) (2 N load)